

Surface plasmons in silver films—a novel undergraduate experiment

H. J. Simon
D. E. Mitchell
J. G. Watson

Department of Physics and Astronomy
The University of Toledo
Toledo, Ohio 43606

(Received 17 October 1974; revised 21 January 1975)

Surface plasmon phenomena are a topic of considerable current interest. We describe a simple experiment and theory for a senior level undergraduate investigation of surface plasmons in silver films. An $\sim 500\text{-\AA}$ -thick silver film is evaporated on the hypotenuse face of a right glass prism. Light (p -polarized) from a He-Ne laser is incident through the prism on the metal film. At an angle of incidence a few degrees greater than the critical angle for total reflection, a sharp minimum in the reflected light is observed, corresponding to the excitation of the surface plasmon. The minimum in the reflectivity results from the absorption of the resonantly enhanced surface plasmon mode in the silver film. The dispersion relation for the surface plasmon and the reflectivity due to the excitation of this normal mode are calculated. Only a modest vacuum of $\sim 10^{-3}$ Torr is necessary to produce the required thin silver films.

INTRODUCTION

Surface plasma waves are transverse magnetic (TM) electromagnetic waves, traveling along the interface of two different media. We will assume one of the media to be a metal and the other to be air. The waves propagate parallel to the interface (along the x direction) and are exponentially attenuated in the normal direction in both the metal and air. The wave vector, k_x , of a surface plasmon on a semi-infinite dielectric bounded by vacuum is given by

$$k_x = \frac{\omega}{c} \left(\frac{\epsilon}{\epsilon + 1} \right)^{1/2}, \quad (1)$$

where ϵ is the complex dielectric function of the medium at the angular frequency ω . For most metals $\epsilon(\omega)$ is less than -1 in the visible region of the spectrum, and we see from Eq. (1) that k_x is greater than the wave vector of an electromagnetic wave in air at the same ω . Surface plasmon waves may be excited only with evanescent waves and are therefore classified as nonradiative. Collective os-

cillations in the electron density at the surface of a metal may be described in terms of these waves.¹

Nonradiative surface plasma waves have been known as solutions of Maxwell's equations since Sommerfeld. The decrease in reflectivity from aluminum films in total internal reflection was first observed by Turbadar; however, he did not attribute this phenomenon to a surface plasmon resonance.² The excitation of the surface plasmon mode in silver films was first recognized by Otto using the method of attenuated total reflection where the evanescent wave is either coupled from the prism into the metal through a thin air spacing, or directly coupled from the prism into a thin metal film.³ Agarwal has described these waves as surface polaritons, corresponding to those solutions of Maxwell's equations which are subject to the Ewald-Oseen extinction theorem with no incident field.⁴ Recently, the present authors have shown that excitation of the surface plasmon mode in silver films enhances the production of optical second-harmonic generation.⁵

We divide our discussion into three sections. First, we describe the surface plasmon mode and derive the dispersion relation given by Eq. (1). Next, we describe the excitation of this mode by the method of attenuated total reflection. Emphasis is placed on the absorption of the enhanced internal optical fields in the metal film for producing the observed minimum in reflectivity. In the final section, we describe the experimental apparatus and discuss typical results that can be obtained from silver films evaporated at pressures as high as 10^{-3} Torr. We conclude by suggesting extensions of this experiment to study surface plasmons in other metals and the dispersion of the surface plasmon.

SURFACE PLASMON DISPERSION

We now derive a dispersion relation that will relate the propagation vector of a surface wave traveling along the surface of a metal to its angular frequency. We consider the space $z > 0$ to be filled with a metal with complex dielectric function $\epsilon = \epsilon_1 + i\epsilon_2$. The real part of the dielectric constant for a free electron metal is given by $\epsilon_1 = 1 - \omega_p^2/\omega^2$, where ω_p is the bulk plasmon frequency.⁶ The imaginary part of the dielectric constant describes the optical absorption processes in the metal. We will assume $\epsilon_2 \equiv 0$ for the purpose of discussing ideal surface plasmon dispersion. The space for $z < 0$ is assumed to be air of dielectric constant unity. The essential assumption is to postulate the existence of only a single wave on each side of the boundary. The electric fields are assumed to be monochromatic plane waves:

$$\mathbf{E}(x, z, t) = \mathbf{E} \exp[i(\omega t - k_x x - k_z z)]. \quad (2)$$

The complete wave equation for this wave in each region may now be written. Normally, in studying wave propagation in an infinite solid, one takes k_x and k_z to be given real numbers and uses the wave equation to determine the frequency of the propagating wave. Instead of this procedure, we assume that ω is given and k_x is a real number

to be determined.⁷ For surface waves we are interested in the conditions under which there are no propagating waves in either the metal or air. We assume ω and k_x have values such that in the metal the solution of the wave equation can be written

$$k_z = -i(k_x^2 - \epsilon\omega^2/c^2)^{1/2} \quad (3a)$$

and in air

$$k_z = +i(k_x^2 - \omega^2/c^2)^{1/2}. \quad (3b)$$

The signs are chosen so that the electric fields in the metal and dielectric describe exponential decay normal to the boundary. In metals this condition is easily satisfied in the visible region of the spectrum where $\omega < \omega_p$; in air this condition is satisfied only for evanescent waves in total internal reflection.

The boundary conditions at the plane $z = 0$ are the standard ones: continuity of the tangential component of \mathbf{E} and \mathbf{H} and of the normal component of \mathbf{D} and \mathbf{B} . We assume the magnetic permeability is equal to unity, and \mathbf{B} is equal to \mathbf{H} . The two transverse modes can be classified by their polarizations, namely, with electric field \mathbf{E} parallel or perpendicular to the plane of incidence defined by k_x and the z axis. For the case in which $E_x = E_z = 0$, s -polarization, no plasma mode solution is found. The case of interest is $E_y = 0$, p -polarization. Now, using continuity of the tangential component of \mathbf{E} and transversality of the fields, we have

$$k_x E_x \Big|_{z=0^+} = k_x E_x \Big|_{z=0^-}. \quad (4)$$

Combining the above with continuity of the normal component of \mathbf{D} gives

$$\epsilon \frac{k_x}{k_x} \Big|_{z=0^+} = \frac{k_x}{k_x} \Big|_{z=0^-}. \quad (5)$$

Substitution from Eqs. (3a) and (3b) allows the above condition to be rewritten as the dispersion relation given by Eq. (1).

SURFACE PLASMON EXCITATION

In this section we relate the amplitude of the surface plasmon mode to the exciting incident radiation. An electromagnetic wave in a glass prism is incident on a thin metal film at the hypotenuse face of the prism and at an angle of incidence greater than the critical angle for total internal reflection. The attenuated total reflection geometry is shown in Fig. 1. We assume the electric field vectors are p -polarized and described by monochromatic plane waves. In the glass medium we have an incident and reflected propagating wave of the form

$$\mathbf{E}_{\text{incident}} = \mathbf{E}_1^i \exp[i(\omega/c)n(x \sin\theta_1 - z \cos\theta_1)] \quad (6a)$$

and

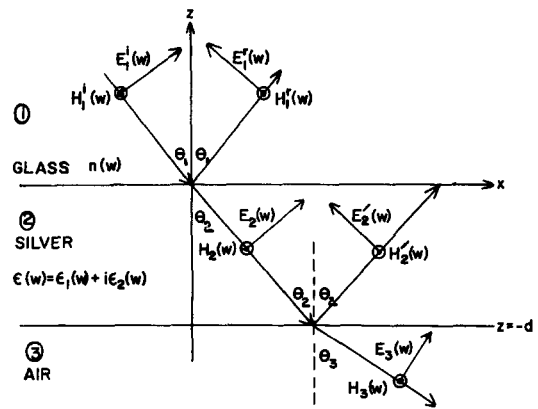


Fig. 1. Attenuated total reflection geometry for a thin metal film between a glass prism and air.

$$\mathbf{E}_{\text{reflected}} = \mathbf{E}_1^r \exp[i(\omega/c)n(x \sin\theta_1 + z \cos\theta_1)]. \quad (6b)$$

In the thin metal film we write the total electric field as a standing wave superposition of two exponentially damped waves:

$$\mathbf{E}_{\text{metal}} = \mathbf{E}_2 \exp[i(\omega/c)nx \sin\theta_1] \exp(kz) + \mathbf{E}_2' \exp[i(\omega/c)nx \sin\theta_1] \exp(-kz). \quad (6c)$$

The transmitted wave in the vacuum is assumed evanescent:

$$\mathbf{E}_{\text{transmitted}} = \mathbf{E}_3 \exp[i(\omega/c)nx \sin\theta_1] \times \exp[(\omega/c)(n^2 \sin^2\theta_1 - 1)^{1/2}z]. \quad (6d)$$

Here k is the absorption coefficient at nonnormal incidence, which by comparison with Eqs. (2) and (3a) is written for the geometry of Fig. 1 as

$$k = -i(\omega/c)(\epsilon - n^2 \sin^2\theta_1)^{1/2}, \quad (7)$$

where ϵ is the complex dielectric coefficient of the metal, as before, n is the index of refraction of the glass, and θ_1 is the angle of incidence. The x dependence of all the waves follows from Snell's law.

The four unknown amplitudes E_1^r , E_2 , E_2' , and E_3 can be related to the incident amplitude E_1^i through the boundary conditions. Continuity of the tangential components of \mathbf{E} and \mathbf{H} at the $z = 0$ and $z = -d$ boundaries gives the required four equations. We thus find the amplitude of the fields in the metal at $z = 0$ to be

$$E_2 = E_1^i \frac{t_{12}}{1 + r_{12}r_{23} \exp(-2kd)} \quad (8a)$$

and

$$E_2' = E_1^i \frac{t_{12}r_{23} \exp(-2kd)}{1 + r_{12}r_{23} \exp(-2kd)}. \quad (8b)$$

The Fresnel reflection and transmission amplitude factors,⁸ with the 12 and 23 subscripts for the glass-metal and metal-air boundaries, respectively, are given by

$$t_{12} = \frac{2n \cos \theta_1}{\epsilon^{1/2} \cos \theta_1 + n \cos \theta_2}, \quad (9a)$$

$$r_{12} = \frac{\epsilon^{1/2} \cos \theta_1 - n \cos \theta_2}{\epsilon^{1/2} \cos \theta_1 + n \cos \theta_2}, \quad (9b)$$

and

$$r_{23} = \frac{\cos \theta_2 - \epsilon^{1/2} \cos \theta_3}{\cos \theta_2 + \epsilon^{1/2} \cos \theta_3}. \quad (9c)$$

The angles θ_2 and θ_3 in the metal and air, respectively, are defined by

$$\cos \theta_2 = (1 - n^2 \sin^2 \theta_1 / \epsilon)^{1/2} \quad (10a)$$

and

$$\cos \theta_3 = (1 - n^2 \sin^2 \theta_1)^{1/2}. \quad (10b)$$

The complex nature of these angles reflects the real exponential decay of the fields in the metal and air media.

We now solve for E_1^r and find the ratio of the reflected optical power to the incident optical power to be given by

$$R = \left| \frac{r_{12} + r_{23} \exp(-2kd)}{1 + r_{12} r_{23} \exp(-2kd)} \right|^2. \quad (11)$$

The critical factor in the above formula is r_{23} , which may be rewritten as

$$r_{23} = \frac{(n^2 \sin^2 \theta_1 - \epsilon)^{1/2} - \epsilon(n^2 \sin^2 \theta_1 - 1)^{1/2}}{(n^2 \sin^2 \theta_1 - \epsilon)^{1/2} + \epsilon(n^2 \sin^2 \theta_1 - 1)^{1/2}}. \quad (12)$$

For an ideal free electron plasma, the denominator of r_{23} vanishes at the plasmon angle θ_p given by

$$n \sin \theta_p = [\epsilon / (\epsilon + 1)]^{1/2}, \quad (13)$$

which is also the condition for the surface plasmon mode given by Eq. (1). The divergence of r_{23} at the surface plasmon resonance was recognized by Cardona⁹ and can be described as the ratio of a finite-amplitude reflected field to a zero-amplitude incident field at the metal-air interface. A more direct interpretation, without any divergent factors, is to recognize directly from Eq. (8a) that when $\theta_1 = \theta_p$ then $E_2 \equiv 0$ and the only field in the metal has a simple exponential spatial decay from the metal-air boundary to the metal-glass boundary. This description is consistent with the surface plasmon mode discussed previously and the surface polariton modes of Agarwal.⁴

The effect of the surface plasmon resonance on the

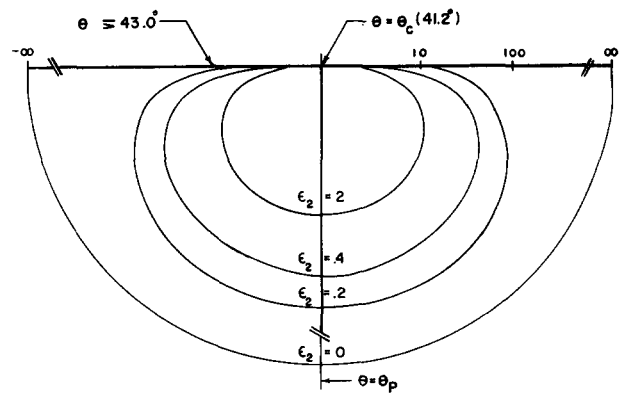


Fig. 2. Polar plot of the complex Fresnel reflection factor, r_{23} , at the silver-air interface for angles of incidence around the plasmon angle. The amplitude scale is logarithmic.

linear reflectivity can be observed only for the case of nonzero absorption given by $\epsilon_2 \neq 0$. [If $\epsilon_2 = 0$, the reflectivity calculated from Eq. (11) remains unity for all angles of incidence including the surface plasmon resonance; however, in nonlinear optics the surface plasmon resonance may still be observed through enhanced harmonic generation.⁵] The plasmon angle θ_p is still defined by the real part of Eq. (13), but r_{23} now assumes a large negative imaginary value. The amplitude and phase of r_{23} in the complex plane as a function of the angle of incidence is plotted in Fig. 2 with a logarithmic amplitude scale. At the critical angle for total internal reflection ($n \sin \theta_c = 1$), we have $r_{23} \approx 1$, but at the plasmon angle $r_{23} \approx -i2\epsilon_1/\epsilon_2$, and beyond this angle r_{23} rapidly approaches ≈ -1 . The amplitude and phase of r_{23} are a sensitive function of the

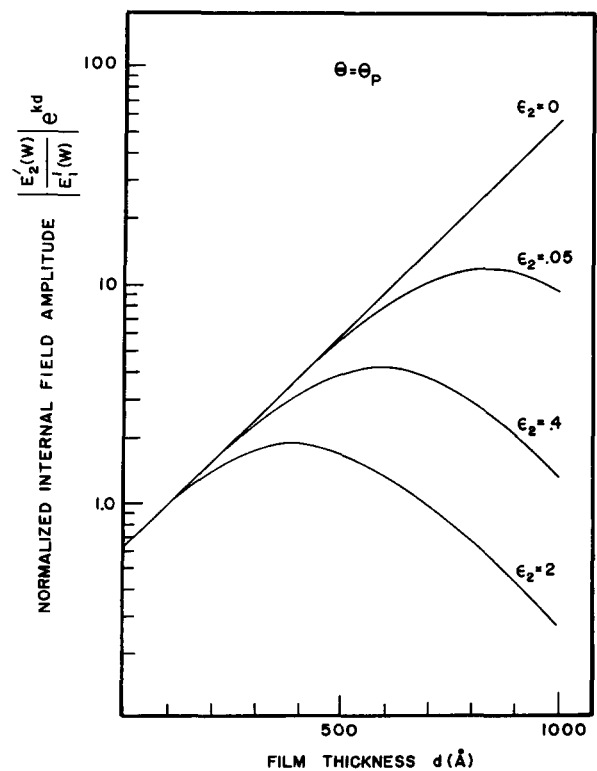
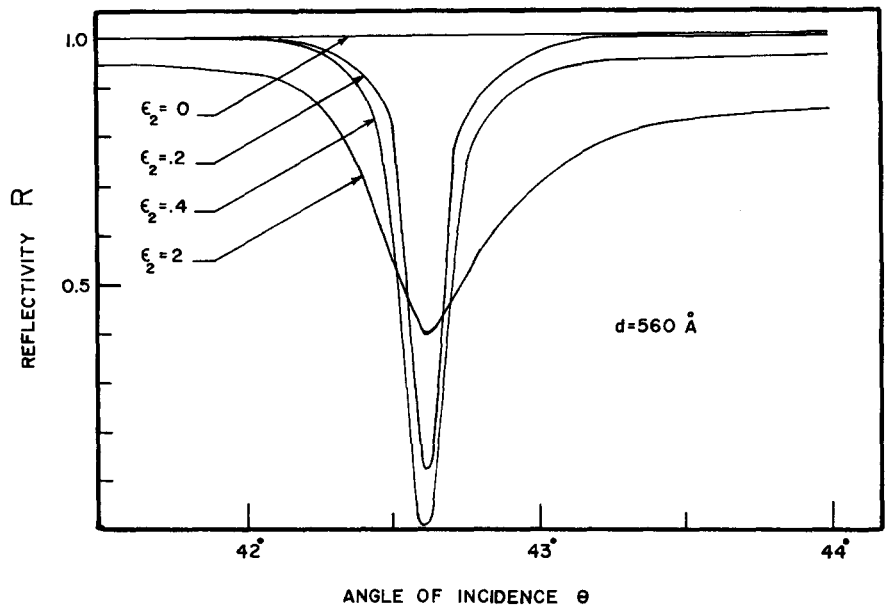


Fig. 3. Normalized amplitude of the surface plasmon mode electric field evaluated at the silver-air interface versus film thickness.

Fig. 4. Reflectance of the surface plasmon mode versus angle of incidence for fixed film thickness and variable absorption constant.



angle of incidence in this region.

In Fig. 3 we display the normalized amplitude of the surface plasmon mode electric field at the plasmon angle evaluated at the metal-air boundary as a function of metal film thickness for several values of ϵ_2 . Note the amplitude scale is logarithmic. For zero absorption the amplitude of this field increases exponentially with the thickness of the film; however, for nonzero absorption this internal field amplitude reaches a maximum, which may be an order of magnitude larger than the incident field. By comparison the normalized amplitude of the other field in the metal film for zero absorption is identically zero, as previously discussed; however, for finite absorption this field is nonzero, although it is still several orders of magnitude smaller than the surface plasmon mode field shown in Fig. 3.

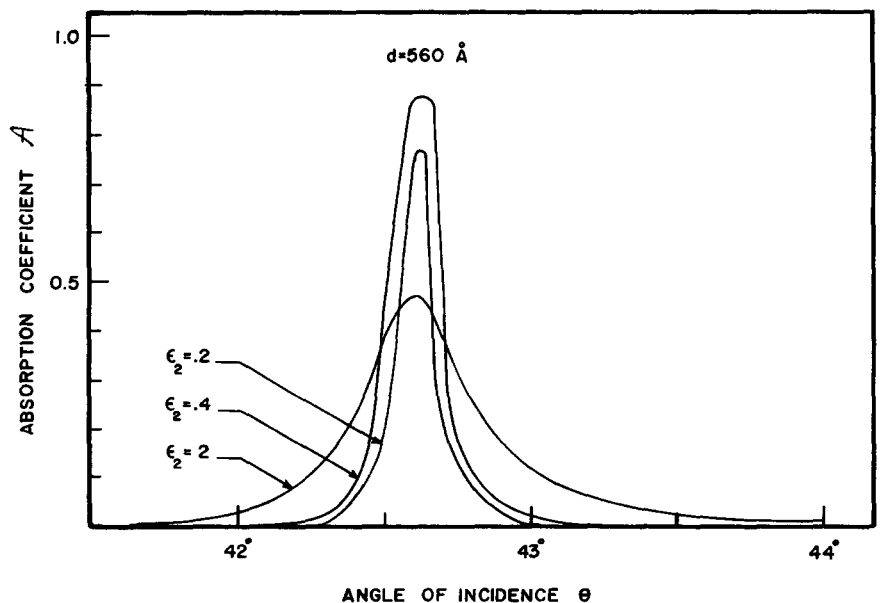
The quantity of experimental interest is the reflectance which is shown in Fig. 4 as a function of the angle of incidence for a fixed film thickness. Again for zero absorption the reflectivity is unity but decreases sharply near

the plasmon resonance as the absorption increases. Note that the angular half-width of these resonant curves increases with absorption. For large values of absorption, the plasmon resonance is heavily damped and the reflectivity minimum is no longer sharp. The effect of damping on the surface plasmon resonance has been discussed by several authors.¹⁰ The reflectivity minimum at the plasmon resonance is due to the increased absorption of the enhanced internal fields throughout the volume of the metal film. Integrating the power absorption density over the irradiated volume of the film and normalizing by the incident power, we have the enhanced absorptance due to the surface plasmon, given by

$$A = \frac{\epsilon_2 \omega [\exp(2kd) - 1] \cos \theta_2}{nc 2k \cos \theta_1} \left| \frac{E_2'}{E_1^i} \right|^2 \quad (14)$$

The above quantity is plotted in Fig. 5. Clearly, the maxima in the absorptance match the minima in the reflectance

Fig. 5. Absorptance of the surface plasmon mode versus angle of incidence for fixed film thickness and variable absorption constant.



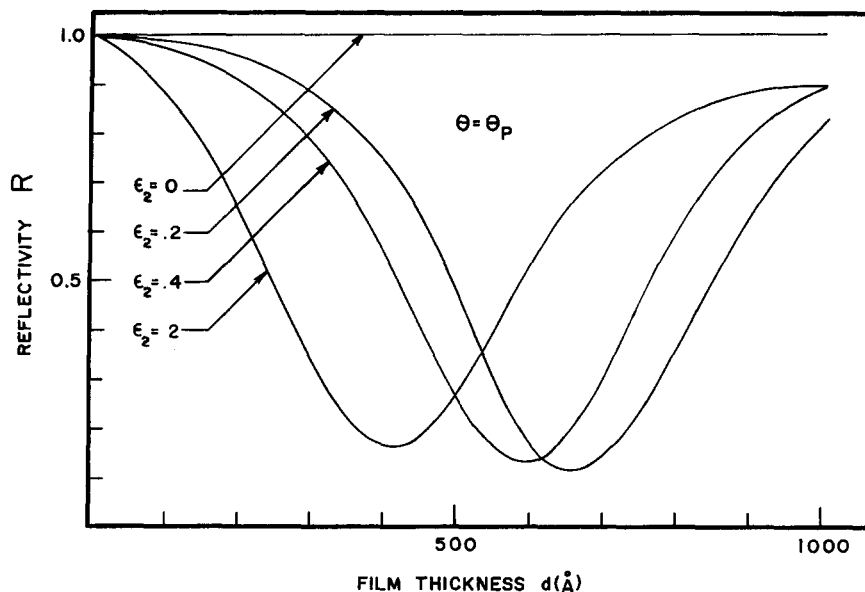


Fig. 6. Reflectance of the surface plasmon mode at the plasmon angle versus film thickness for variable absorption constant.

tance. In Fig. 6 we show the reflectance at the plasmon angle as a function of film thickness in order to estimate the optimum film thickness in the following section.

EXPERIMENT AND RESULTS

In this section we describe a simple apparatus for evaporating thin silver films, discuss the experimental results, and make suggestions for further experiments. Our apparatus which produced a vacuum of 10^{-3} Torr consisted of an Edwards 3-in. diffusion pump connected to a Vector 75 rotary roughing pump and a 6-in. bell jar with a No. 8 rubber stopper at its top through which the two electrodes entered the vacuum chamber. A coiled filament basket was made from tungsten or molybdenum wire. A 1.5-cm length of 99.999% silver wire¹¹ (1-mm diameter) was placed at the bottom of the coil which was attached to the electrodes. Before the prism was placed at the bottom of the bell jar, the hypotenuse face was cleaned with reagent grade methanol and rinsed with distilled water. A metal shutter, magnetically coupled to the outside of the bell jar, was placed between the silver and the prism to block any impurities that might boil off while the silver was initially heated. A sketch of this apparatus is shown in Fig. 7. A current of 4–8 A supplied by a Variac caused the filament to gradually glow red hot and the silver to slowly melt into a small ball at the bottom of the filament. The shutter was then opened and the coating process begun. After a few minutes of evaporation, the current was turned off and the pressure inside the bell jar was returned to atmospheric.

The prism was then removed from the evaporator and placed on a suitable rotary platform or a student grade spectrometer. A He-Ne laser beam polarized in the plane of incidence by a Polaroid sheet was incident on the prism, and the reflected beam could initially be observed on a white piece of paper. At the critical angle for total internal reflection, the reflected intensity approximately equaled the incident intensity, but as the external angle of incidence was increased by 2° – 3° , the reflectivity was observed first to decrease sharply and then to increase again. A simultaneous increase in the scattered-light intensity from the laser spot on the back silver-air surface

was also observed. When the reflected light was detected with a RCA 1P28 photomultiplier whose output was measured with a voltmeter, the results shown in Fig. 8 were obtained. The minimum in reflected intensity observed in this experiment was comparable to the extinction obtained with crossed polarizers.

The only experimental technique requiring a little experience is coating the correct film thickness. Referring to Fig. 6, we see that films either less than 300 Å thick or greater than 800 Å thick will produce shallow reflectivity

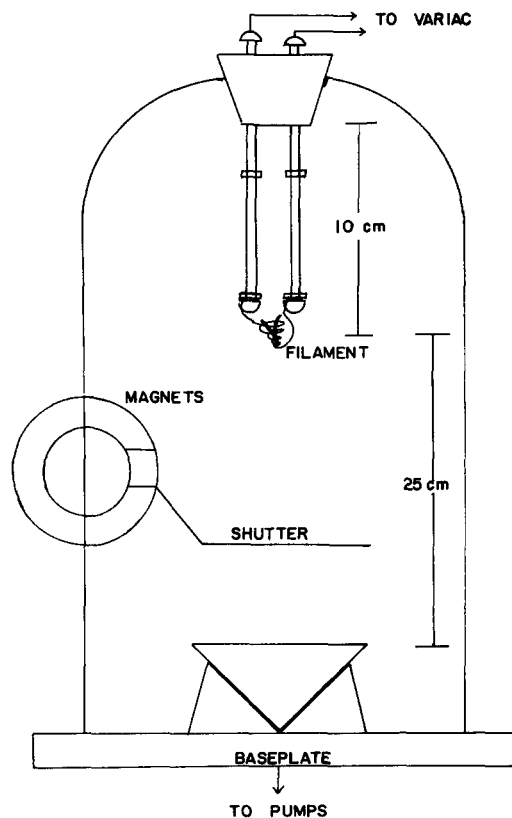
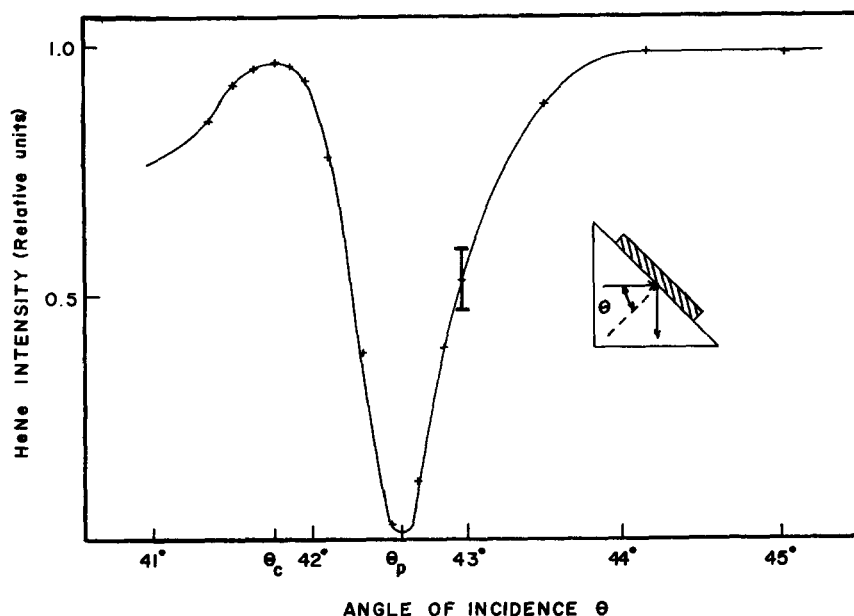


Fig. 7. Sketch of simple evaporator apparatus. Prism with hypotenuse face up rests on the base plate.

Fig. 8. Experimental reflectance of the surface plasmon mode versus angle of incidence in a silver film 560 Å thick on a crown glass prism at the He-Ne laser wavelength 6328 Å.



minima. When viewed from the hypotenuse face, too thick a film will appear opaque while too thin a film will appear semitransparent; however, the apex edge of the prism should be visible through the metal film. If the surface plasmon resonance is not observed, the prism should be recleaned and the evaporation process repeated again. Since this process requires only a few minutes, new samples of varying thickness may be easily prepared until the desired effect is achieved. Film thickness may be determined by placing a microscope slide adjacent to the prism surface in the evaporator and measuring the optical transmission of the coated slide. For the 560-Å film used in this experiment, the transmission of the slide was approximately 1% at 6328 Å.

The numerical calculations for the curves presented in Figs. 2–6 were performed on a PDP-11 time-sharing computer. The complex dielectric constant of the silver film¹² was $\epsilon = -18.3 + i0.4$ at the He-Ne laser wavelength (6328 Å), and the index of refraction of the crown glass prism was taken to be $n = 1.52$. The optical properties of the silver film are sensitive to the conditions of film preparation (especially at our vacuum pressure of 10^{-3} Torr) and to the growth of silver sulfide layers on the film in air¹³; therefore, the value of ϵ_2 was allowed to take on a wide range of values to test the sensitivity of the reflectance to this parameter. We see from Fig. 4 that the qualitative features of the reflectivity minimum should be observable over a large range of ϵ_2 . The results displayed in Fig. 8 were repeatable with the same film maintained in the ambient laboratory environment over a period of several weeks. Although the films should be evaporated under high vacuum (10^{-9} Torr) and remain in vacuum during the experiment, such stringent conditions are not necessary for the qualitative observation of surface plasmon phenomena.

There are several interesting extensions of this experiment. One experiment is to replace the He-Ne laser source, which was chosen solely for its experimental convenience, with a collimated monochromator. By measuring the angle at which the reflectivity minimum occurs as a function of wavelength, one can experimentally determine the dispersion relation for the surface plasmon. This curve

may then be compared with Eq. (1). The observed back bending in the near ultraviolet of this experimentally determined dispersion curve is a result of the damping of the surface plasmon.¹⁰ Another experiment is to use other metals which can be easily evaporated, for example, aluminum, gold, and copper. The relevant parameter for estimating the strength of the surface plasmon resonance is the magnitude of the ratio ϵ_1/ϵ_2 . For silver in the near infrared, this ratio is larger than that of the other metals.¹⁴ The sharpest reflectivity minima will now occur for smaller film thicknesses than in silver. For an aluminum film, Turbadar² gives a thickness of 125 Å at a wavelength of 5500 Å. The dispersion of surface plasmons in gold films has been studied by Barker.¹⁵ The opportunity exists to make original observations of the surface plasmon resonance in many metals by use of the technique we have described here.

In conclusion, we have given a theoretical description of the effect of the surface plasmon mode on the reflectivity of thin metal films and have demonstrated how such films may be prepared with a modest apparatus. The dramatic change in reflectivity of a silver film should not only provide a stimulus in the laboratory for physics students, but should also provide a dramatic effect in a lecture demonstration for a more general audience.

¹For a review of surface plasmon physics, see R. H. Ritchie, *Surf. Sci.* **34**, 1 (1973).

²T. Turbadar, *Proc. Phys. Soc. Lond.* **73**, 40 (1959).

³A. Otto, *Z. Phys.* **216**, 398 (1968); *Phys. Status Solidi* **42**, K37 (1970).

⁴G. S. Agarwal, *Phys. Rev. B* **8**, 4768 (1973).

⁵H. J. Simon, D. E. Mitchell, and J. G. Watson, *Phys. Rev. Lett.* **33**, 1531 (1974).

⁶C. Kittel, *Introduction to Solid State Physics* (Wiley, New York, 1967), 3rd ed., p. 233.

⁷K. W. Chiu and J. J. Quinn, *Nuovo Cimento B* **10**, 1 (1972). This reference contains a generalized derivation of the surface plasmon dispersion relation.

⁸M. Born and E. Wolf, *Principles of Optics* (MacMillan, New York,

1965), 3rd ed., p. 62.

¹M. Cardona, Am. J. Phys. **39**, 1277 (1971).

²E. T. Arakawa, M. W. Williams, R. N. Hamm, and R. H. Ritchie, Phys. Rev. Lett. **31**, 1127 (1973); R. W. Alexander, G. S. Kovenor, and R. J. Bell, Phys. Rev. Lett. **32**, 154 (1974).

³Metals and evaporator supplies may be obtained from Electronic Space Products, 854 So. Robertson Blvd., Los Angeles, CA 90035.

¹²P. B. Johnson and R. W. Christy, Phys. Rev. B **6**, 4370 (1972).

¹³J. M. Bennet, J. L. Stanford, and E. J. Ashley, J. Opt. Soc. Am. **60**, 224 (1970).

¹⁴American Institute of Physics Handbook (McGraw-Hill, New York, 1963), 2nd ed., Sec. 6-g.

¹⁵A. S. Barker, Jr., Phys. Rev. B **8**, 5418 (1973); Am. J. Phys. **42**, 1123 (1974).

J or psi
(a physicist's four-footed sonnet)

*Where is the thing beneath the thing?
When can we say we have found it all?
Is there an end or just a string
That dangles down like an endless fall?*

*Molecules, yes, and atoms, too,
Electrons we know, and nuclei;
Neutrons, protons, the particle zoo,
And enter now the J or psi.*

*Can we not try to knot the string,
To start from a bottom and see what grows?
Plant us a seed and see what we get
When unity doubles and does its thing
And triples, quadruples, quintuples. Who knows
What patterns will show? What world is there yet?*

—Roger E. Clapp